TÜBİTAK

Turkish Journal of Veterinary and Animal Sciences

http://journals.tubitak.gov.tr/veterinary/

Research Article

Turk J Vet Anim Sci
(2017) 41: 656-666

doi:10.3906/vet-1702-48

Gene cloning and expression analysis of mitochondrial glutathione reductase from Arabian camel (*Camelus dromedarius*) liver in Escherichia coli

Mona ALHARBI*, Abdulrahman ALSENAIDY, Sooad ALDAIHAN, Anwar AHMED
Department of Biochemistry, College of Science, King Saud University, Riyadh, Saudi Arabia

Received: 21.02.2017 • **Accepted/Published Online:** 17.08.2017 • **Final Version:** 13.11.2017

Abstract: Glutathione reductase (GR) is highly conserved among diverse taxa and has important biochemical functions. These functions may facilitate survival in harsh conditions, but the role of GR from the liver of the Arabian camel (*Camelus dromedarius*) is unknown. In this study, the mitochondrial glutathione reductase gene (*Gsr*) from *C. dromedarius* liver was cloned and highly expressed in *Escherichia coli* (Jm109) to gain insight into GR functions in the liver. After amplification of the cDNA encoding the functional unit of *Gsr* (1.2 kb), the products were cloned into the PGEM-T Easy and PET28a vectors. *Gsr* expression was confirmed using an immunoblotting technique (45 kDa). Recombinant GR was purified to homogeneity using Ni-NTA resins, with an overall yield of 7.23% and a specific activity of 0.3063 U/mg. The optimum pH of recombinant GR was 7 and the optimum temperature was 35 °C in 50 mM K_3PO_4 buffer. The Michaelis constant, K_m, for the substrates glutathione disulfide (GSSG) and NADPH was 45.6 µM and 63.5 µM, respectively; moreover, maximal velocity (V_{max}) values were 3.969×10^{-2} U/mg and 1.497×10^{-1} U/mg. This partial characterization of camel liver GR extends our insight into the ability of camels to cope with harsh environmental conditions.

Key words: *Camelus dromedaries* liver, pGEM-T Easy vector, Ni-NTA resin, recombinant glutathione reductase, partial characterization

1. Introduction

Glutathione reductase (GR) (E.C.1.8.1.7), a flavoenzyme in the family of pyridine nucleotide-disulfide oxidoreductases, induces a hydrogen transfer from NADPH to oxidized glutathione (GSSG) in order to maintain a high level of reduced glutathione (GSH). The enzyme is crucial for the maintenance of a high intracellular ratio of reduced glutathione to the oxidized form (1,2). The reaction that converts GSSG to GSH is fast and irreversible (see reaction below); thus, the enzyme ensures a high ratio of intracellular reduced glutathione to the oxidized form, estimated at 300:1 (3–5).

$$GSSG + H^+ + NADPH \leftrightarrow 2GSH + NADP^+$$

GSH is an essential antioxidant (6) and is a significant intracellular thiol composite involved in the thiol reduction-oxidization state, which is associated with various biochemical processes, such as protein assembly, phosphorylation, protein structural stability, cysteine residue protection, DNA transcription factor activity, and the acceleration of H_2O_2 scavenging in the redox pathway (7,8). As an enzyme in the glutathione reduction-oxidization cycle, GR is a cell safeguarding mechanism and shields cells from the harmful effects of internal and external sources of hydrogen peroxide. It is taxonomically widely distributed (9,10). GR deficiency causes blood cell damage owing to an elevated sensitivity of the red blood cell envelope to hydrogen peroxide; in addition, it causes an elevation in the levels of free radicals, which are involved in the pathogenesis of many diseases (6,11). Changes in GSH levels cause oxidative stress on intercellular/intracellular surfaces (2). GR is vital for controlling the intracellular balance between reduced glutathione and the oxidized form, the degree of damage to mitochondria and chloroplasts, and the ability of cells to protect against external and internal stress factors (12,13).

GR differs slightly among taxa with respect to its physical characteristics and substrate affinity (i.e. GSSG). GR isoforms from both prokaryotes and eukaryotes form stable homodimers of ~110 kDa with a large subunit interface of more than 3000 Å^2. GR has been purified from multiple sources, e.g., calf livers (14), rodent livers (15), human red blood cells (16), sheep brains (17), sheep livers (18), turkey livers (19), and *Chlamydomonas reinhardtii* (20), and its characteristic properties, such as its thermostability, optimal pH, and optimal temperature, have been characterized. Affinity chromatography, ion exchange chromatography, hydrophobic and reversed-phase chromatography, and size exclusion chromatography have been applied in order to purify the enzyme (21–24).

* Correspondence: moshujaa@ksu.edu.sa

Deserts are characterized by high temperatures and conditions that induce dehydration and low nutrient levels. However, the Arabian camel (*Camelus dromedarius*) has the ability to tolerate extremely dry and hot desert environments. The distinctive physiological and biochemical functions of camel cells play a principle role in organismal adaptation to heat and dehydration. Based on the broad functions of GR, and particularly its role in stress responses, it may be important for the survival of camels in harsh conditions. In the current study, we cloned, expressed, and purified recombinant GR obtained from camel liver to examine the kinetic and physical properties of the enzyme.

2. Materials and methods

2.1. Sample collection and cDNA preparation

An Arabian camel (*C. dromedarius*) liver was collected from a local slaughterhouse and placed in a liquid nitrogen and RNA*later* solution (RNA*later* RNA Stabilization Reagent, QIAGEN) in sterilized plastic bags, which were stored at –80 °C until RNA extraction (AxyPrep Multisource Total RNA Miniprep Kit, Axygen, Union City, CA, USA). First-strand cDNA was synthesized using High Capacity cDNA Reverse Transcription (Applied Biosystems, Carlsbad, CA, USA). The thermal cycle conditions are shown in Table 1.

All applicable international, national, and/or institutional guidelines for the care and use of animals were followed. All of the procedures described were reviewed and approved by the King Saud University Graduate studies on 3 March 2012 (Approval No. 3/2/134296).

2.2. Cloning and PCR sequencing

Primers to amplify the region of the glutathione reductase encoding the functional unit (1.2 kbp) lacking the leader sequence (300 bp) at the N-terminus (GenBank ID at NCBI: KR422694) were based on conserved regions identified by the aligning of glutathione reductase (GR) sequences of *Homo sapiens* (Figure 1). The forward (GSRFor1) and reverse (GSRRev1) primers were designed with XhoI and HindIII restriction sites, respectively (Table 2). Polymerase chain reaction (PCR) amplification for *Gsr* was performed using HotStarTaq Master Mix. The conditions for a thermal cycle are shown in Table 1. Plasmids were extracted using a QIAGEN Plasmid Miniprep Kit (QIAGEN GmbH, Germany). The PCR products were separated by 1% agarose gel electrophoresis, isolated from the gel using Wizard SV Gel and PCR Clean-Up System Solutions (Promega, Fitchburg, WI, USA), and cloned in a TA cloning vector (pGEM-t Easy) (Promega) to create the *Gsr*-pGEM-t plasmid. *E. coli* JM109 competent cells were prepared by $CaCl_2$ and transformation was done by heat shock method (25). The plasmids were propagated in *E. coli* strain JM109 (New England Biolabs Inc.) in Luria-Bertani (LB) medium (10 g NaCl, 10 g Bacto Tryptone, and 5 g yeast extract for 1 L) with 100 µg/mL ampicillin (Sigma-Aldrich) (Amp+/LBion) and media were solidified by addition of 2% agar. The plasmid *Gsr*-pGEM-t was digested using XhoI and HindIII and the 1.2-kbp fragment was cloned into the expression vector pET28a (Novagen, Germany) that was digested with the same restriction enzymes to create the pET23a-*Gsr* plasmid in LB medium containing 50 µg/mL kanamycin (Sigma-Aldrich) (Kan+/LB). All the restriction enzymes were obtained from New England Biolabs Inc. The plasmid PET28a-*Gsr* was sent to the Core Sequencing Facility at the King Faisal Specialist Hospital and Research Center (Riyadh, Saudi Arabia) to confirm the gene sequence.

2.3. Bioinformatic analysis of *Gsr*

Sequence electropherograms were analyzed using Chromas (Version 1.5) (Figure 2). The open reading frame was identified using NCBI/BLAST (available at http://blast.ncbi.nlm.nih.gov/Blast.cgi). A phylogenetic tree of GR family members was constructed using the neighbor-joining method implemented in phylogeny.fr, one-click mode (http://www.phylogeny.fr/) (26).

Table 1. The thermal cycle conditions for cDNA synthesis and amplification of the glutathione reductase gene.

Reaction step	Temperature (°C)	Time
cDNA synthesis Annealing	25	10 min
cDNA synthesis	37	60 min
Denaturation	85	15 min
Amplification of gene		
Initial denaturation	95	15 min
Denaturation × 32 cycles	95	25 s
Annealing × 32 cycles	52.3	30 s
Extension × 32 cycles	72	2 min

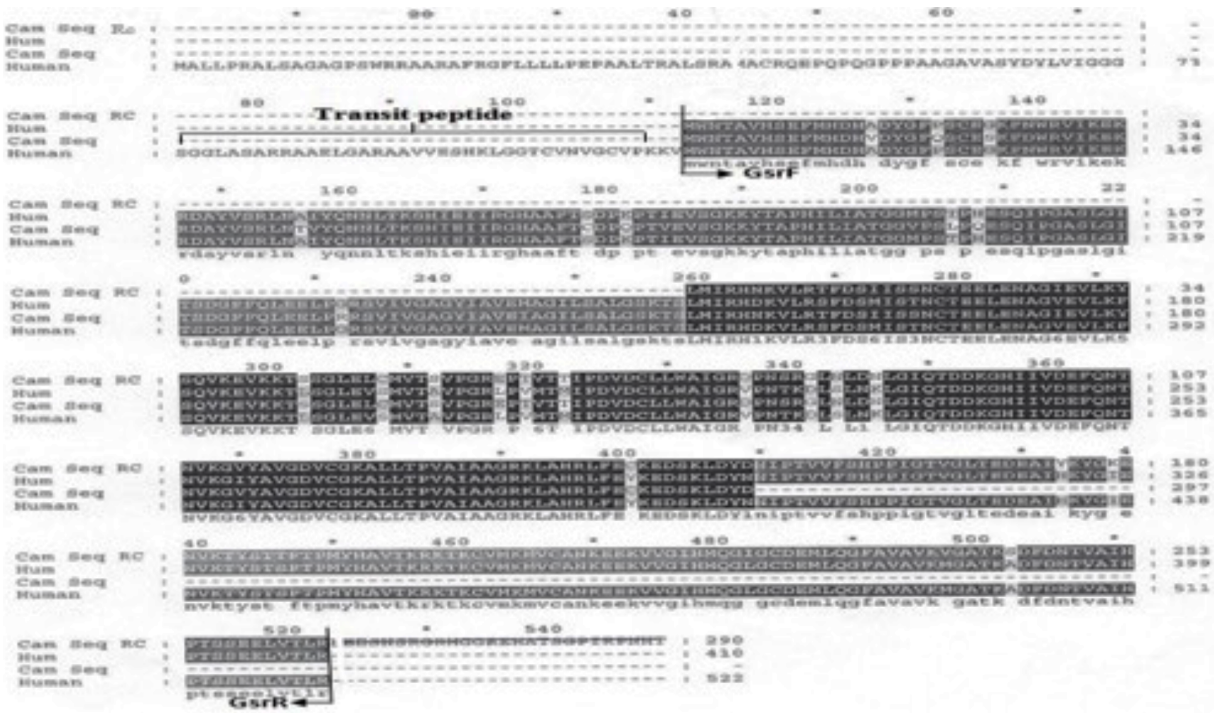

Figure 1. The primer design based on *Homo sapiens Gsr* (Gene ID: 2936), *Gsr* not having a transit peptide (leader sequence) in the N-terminal, Cam Seq Rc: GsrFor1 (forward primer), Cam Seq: GsrRev1 (reverse primer).

Table 2. Forward (GSRFor1) and reverse (GSRRev1) primer sequences.

No..	Primer	Sequence
1	GsrFor1	5'-CAAGCTTCGATGTGGAACACAGCTGTCCACTCTGAATTC-3'
2	GsrRev1	5'-CCTCGAGTCAACGAAGTGTGACCAGTTCTTCTG-3'

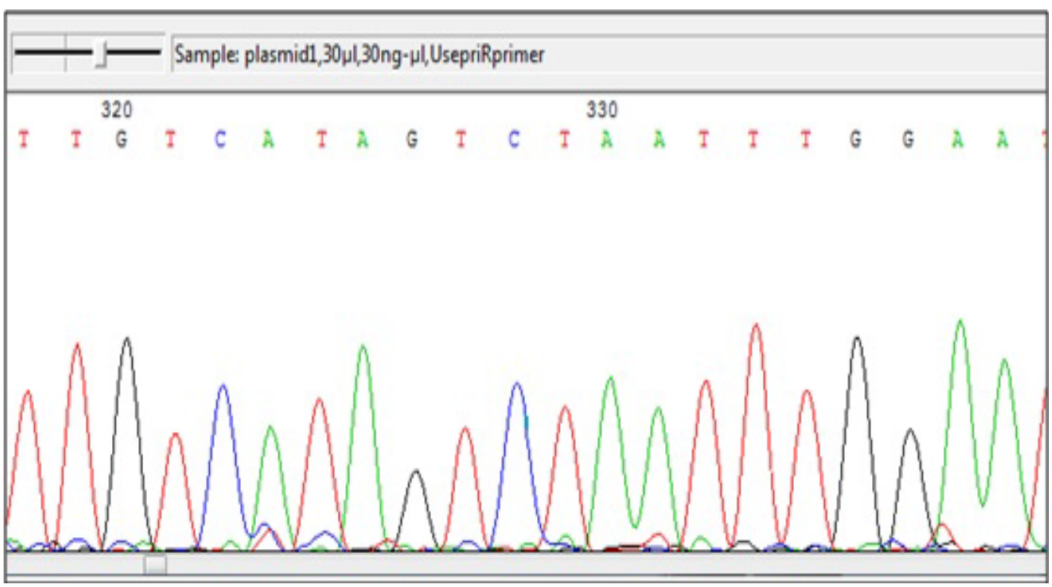

Figure 2. Sequence analysis of 1.2 kbp of *Gsr* using Chromas software.

2.4. Expression of the glutathione reductase gene

For large-scale GR expression, the JM109 (DE3) strain of *E.coli* transformed with pET28a-Gsr was grown for 16 h at 37 °C in 250-mL flasks containing 10 mL of Kan+/LB. This culture was used to inoculate 1 L of Kan+/LB and then grown to an optical density at 600 nm (OD600) of 0.6. Expression of hexahistidine-tagged GR (His6-GR) was then induced by addition of isopropyl-1-thio-β-D-galactopyranoside (IPTG, Sigma-Aldrich) to a final concentration of 1 mM. Cultures were grown at 37 °C for 4 h along with a negative control culture without IPTG (Figure 3).

Expression was analyzed by western blot. The expressed protein (GR) was first observed on SDS-polyacrylamide gel electrophoresis (SDS-PAGE), which was carried out according to the method of Laemmli (27), and then transformed into Amersham Hybond-ECL membrane using a western blotting apparatus at a constant voltage of 100 V for 1 h in cooling conditions at ~4 °C. The membrane was incubated overnight in blocking buffer (3% nonfat milk dissolved in phosphate saline buffer, PSB). The membrane was then washed twice with 1X PSB for 10 min each prior to incubation with the rabbit anti-GSR primary antibody, which was raised against the synthetic peptide (PKPTIEVSGKKYTAPHILIATGGMPSTPHESQIPGASL GITSDGFFQLEE) (1:5000 dilution in 1X PSB) for 2 h at room temperature. The membrane was washed again four times with 1X PSB. The bound antibody was incubated with the HRP-conjugated goat antirabbit IgG antibody (1:5000 dilution in 1X PBS) and the bands were developed using SIGMAFAST DAB with a metal enhancer in deionized water for 10 min.

2.5. Purification of the recombinant glutathione reductase (His-6GR) by affinity chromatography

The His6-GR was purified by Ni-NTA (nitrilotriacetic acid) resin chromatography (QIAGEN) at 4 °C. For optimization, five different lysis buffers were used; all had 50 mM NaH_2PO_4, 300 mM NaCl, and 0.1% Nonidet-P40, but the pH values and final concentrations of imidazole (mM) in the lysis buffers varied (Table 3). The cell suspension was thawed for 15 min, resuspended in 10 mL of respective lysis buffers, and incubated on ice for 30 min. The pellet cells were sonicated (Fisher Scientific Sound Enclosure for Model 50 to 120 Sonic Dismembrator, ten times for 20 s each time with pauses of 30 s in between) and then harvested by centrifugation (11,000 × g at 4 °C for 20 min). The supernatant obtained (~10 mL/1 L cell culture) was mixed with 400 µL of Ni-NTA resin that had previously been equilibrated with 1 mL of the respective lysis buffers for 5 min with rocking at 37 °C. This washing was repeated 3 times for each of the lysis buffers. The clear lysate (supernatant) containing the His6-tagged protein was mixed with the equilibrated Ni-NTA resin and kept rocking at 4 °C for 90–120 min. The resin/lysate mixture was loaded onto a column under gravitational force. The resin was washed using 10 column volumes of Wash Buffer 1 (50 mM NaH_2PO_4, 300 mM NaCl, pH 8) or Wash Buffer 2 (50 mM NaH_2PO_4, 300 mM NaCl, 10 mM imidazole, pH 8) under the influence of gravity. Proteins in lysis buffers 1, 4, and 5 were washed with Wash Buffer 1, and proteins in lysis buffers 2 and 3 were washed with Wash Buffer 2. The recombinant GR was eluted with 2 mL using Elution Buffer 1 (50 mM NaH_2PO_4, 10 mM NaCl, 50 mM imidazole) or Elution Buffer 2 (50 mM NaH_2PO_4, 10 mM

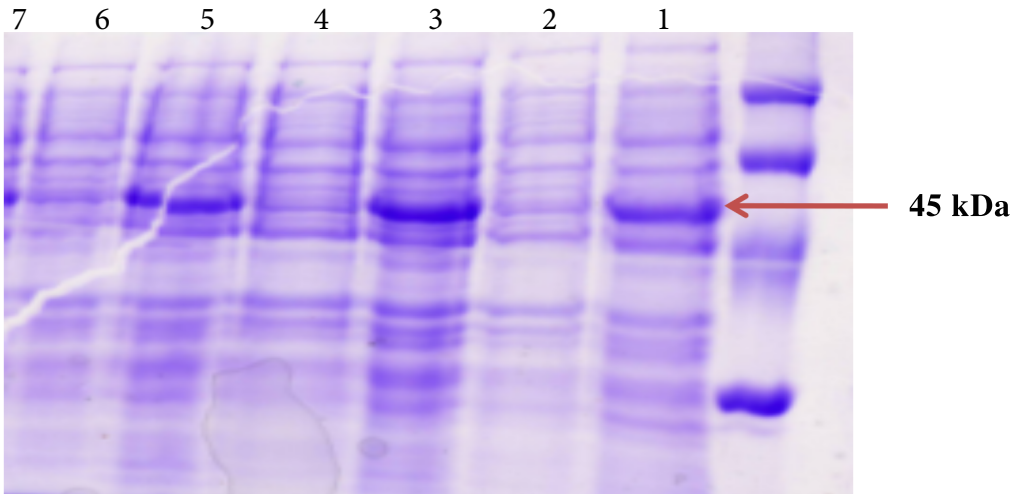

Figure 3. The effect of the IPTG on the efficiency of the induction of pET28a-*Gsr* into JM109 (DE3). Lane 1: Molecular weight marker, 250 kDa; lanes 2, 4, and 6: the cell extract in the presence of 1 mM IPTG; lanes 3, 5, and 7: negative controls without adding inducer.

Table 3. The difference among five lysis buffer preparations.

Lysis buffer	Imidazole, mM	pH
1	-	6
2	-	7.4
3	10	8
4	20	8
5	-	8

NaCl, 300 mM imidazole). To monitor the protein in the collected fractions, absorbance at 280 nm was used. The eluates were dialyzed at 4 °C in 500 mL of dialysis buffer (50 mM NaH_2PO_4, 10% glycerol, pH 7.4) for 4 h. Aliquots of the dialyzed protein were made to 20% in glycerol and stored at –80 °C.

2.6. Kinetics and physical properties

The assay traditionally used for GR was determined spectrophotometrically by following the rate of NADPH oxidation to $NADP^+$ at 340 nm (28). The glutathione reductase was assayed by using a standard assay mixture that contained 50 mM potassium phosphate buffer (pH 7.5), 0.2 mM NADPH, and 0.1 mM GSSG in a final volume of 1 mL. The reaction was initiated by the addition of an appropriate volume of enzyme (10 µL) (29). The protein was estimated by the Bradford method (30) using BSA as a standard solution.

The purified recombinant GR was assayed at different pH values ranging from 5 to 9. Optimum temperature was measured between 25 and 80 °C at a constant pH of 7.5 in 50 mM potassium phosphate buffer. Thermal stability was obtained by incubating the enzyme at 50 °C, 60 °C, and 80 °C for different periods in the same phosphate buffer. The reaction was initiated by adding the substrates at the saturating concentration (0.1 mM GSSG, 0.2 mM NADPH); the graphs for physical properties were created by Microsoft Excel 2013. For kinetics studies, the K_m and V_{max} values were determined from the Lineweaver–Burk plot using GraphPad Prism (version 5.00 for Windows, GraphPad Software, San Diego, CA, USA)

3. Results

3.1. Bioinformatic analysis of *Gsr*

Gsr from the liver of the Arabian camel (*C. dromedarius*) was 1353 bp with a protein-coding sequence of 1201 bp, encoding 401 amino acids. The predicted molecular weight of GR was 41 kDa with an estimated pI of 6.1. As shown in the phylogenetic tree (Figure 4), the GR amino acid sequence of *C. dromedarius* shared the highest sequence identity (99%) with the GR amino acid sequences of *C. bactrianus*, *C. ferus*, and *Vicugna pacos*, followed by the

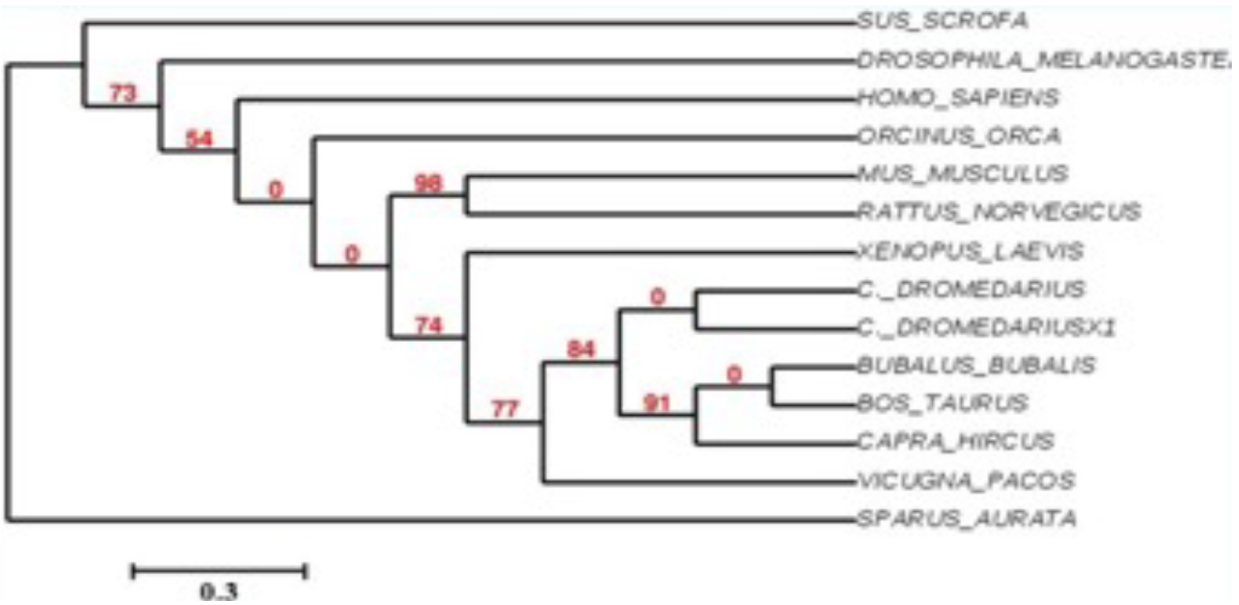

Figure 4. Phylogenetic relationships among GRs of various species generated using the neighbor-joining method implemented in MABL. Tree structure of GR amino acid sequences from *Sus scrofa* (XM_003483642.2), *Drosophila melanogaster* (DMU81995), *Homo sapiens* (BC069244.1), *Orcinus orca* (XM_004277139.1), *Mus musculus* (X76341.2), *Rattus norvegicus* (NM_053906.2), *Xenopus laevis* (NM_001095853.1), *Camelus dromedarius* (KR422694), *Camelus dromedarius* X1 (XM_010987985.1), *Bubalus bubalis* (XM_006076205.1), *Bos taurus* (NM_001114190.2), *Capra hircus* (XM_005698806.1), *Vicugna pacos* (XM_006201146.1), and *Sparus aurata* (AJ937873.2). GenBank accession numbers are in parentheses.

GRs of *Bison bison*, *Bos taurus*, *Ovis aries*, and *Bubalus bubalis*. The expressed GR shared 88% sequence identity with those of *Homo sapiens*, *Dasypus novemcinctus*, and *Callithrix jacchus*. According to the phylogenetic tree, the *C. dromedaries* GR was most closely related to those of the families Camelidae and Bovidae.

3.2. Protein purification

The effect of IPTG concentration on induction efficiency was examined and the results were checked with the DAB method of immunoscreening using the anti-GR antibody produced in rabbit (Figure 5).

In the purification process, lysis buffer 1 yielded the best results. Different elution buffers (E1 and E2) were used to elute the GR and a good result was observed when 50 mM imidazole was used (Figure 6).

3.3. Kinetics and physical properties

GR exhibited a specific activity of 0.306 U/mg. The protein concentrations of the crude extract and pure GR were 3.6 mg/mL and 1.1 mg/mL, respectively. The amount of native enzyme was approximately 4.4 mg. Table 4 shows the purification steps of the GR enzyme. The rate of reaction was calculated by the following formula:

Enzyme activity (U/mL) = $\Delta A_{340} \times$ D.F. / Σ (Σ = 6.22)

Kinetic parameters were determined for purified GR. Line equations derived from the Lineweaver–Burk plot were used to calculate the K_m values for GSSG (Figure 7A) and NADPH (Figure 7B), which were 45.6 µM and 63.5 µM, respectively.

The optimum pH observed over a broad range and with maximum activity was approximately 7 (Figure 8A). As displayed in Figure 8B, the maximum enzyme reaction rate was observed at 35 °C. Nevertheless, enzyme reaction rates dropped strongly for temperatures of 60 °C to 70 °C. Accordingly, the optimal temperature for the GR reaction was 35 °C.

Regarding the thermostability, the enzyme showed activity at 50 °C and was inactivated at high temperatures (60 °C and 80 °C; Figure 8C).

4. Discussion

GR affects organismal responses to environmental stresses, such as direct sunlight and harsh desert conditions, and accordingly may be important for camel health (31). In the present study, GR from the *C. dromedarius* liver was purified and partially characterized.

Physiological conditions have a large influence on protein expression in general. For example, *E. coli* yields higher protein quantities when grown at 30 °C than at 37 °C (32); however, in our analysis, 37 °C was optimal for *Gsr* expression.

For functional and kinetic analyses, large quantities of recombinant protein are required. Accordingly, it is

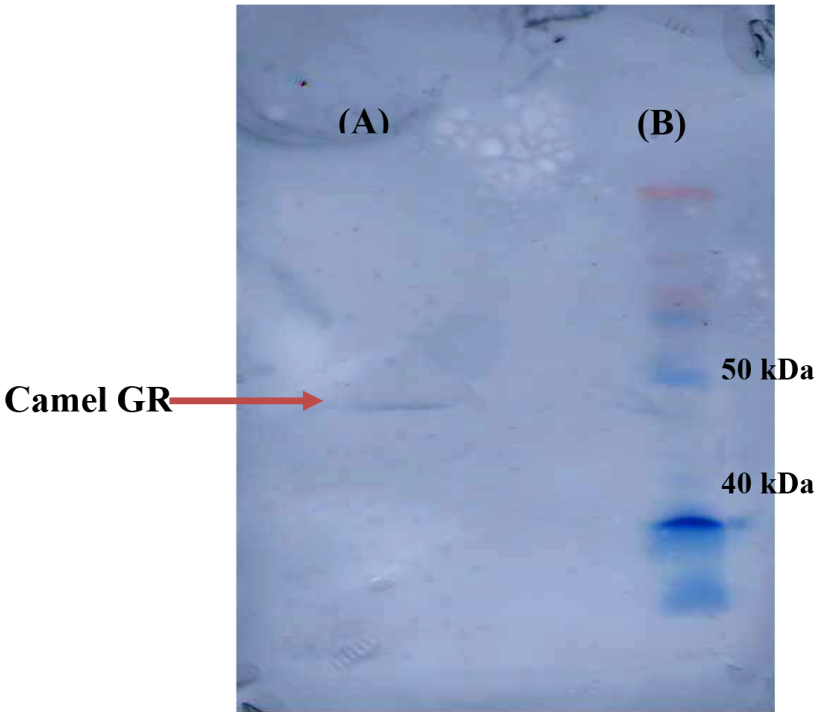

Figure 5. Soluble GR protein was subjected to western blot analyses with the GR antibody at a dilution of 1:5000. The arrowhead indicates the position of GR (~45 kDa). Lane A shows purified GR (0.5 µg). Lane B: a set of protein markers (14–100 kDa).

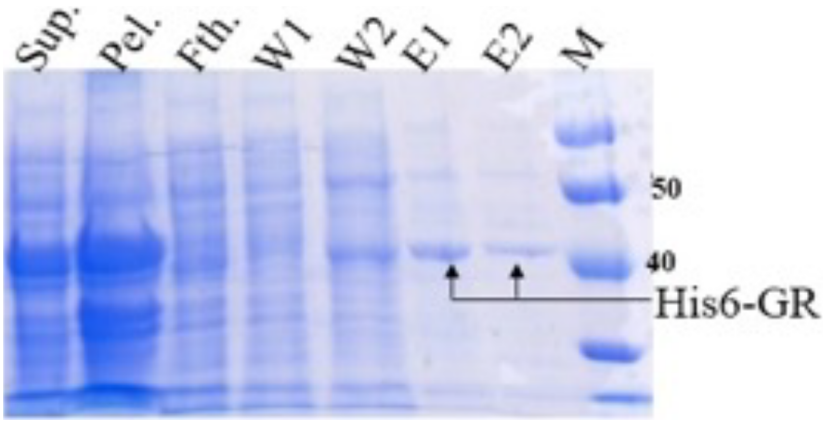

Figure 6. Purification of recombinant glutathione reductase (His6-GR). Recombinant GR was expressed in *E. coli* and indicated fractions were analyzed by SDS-PAGE with a 14–100 kDa protein marker (M). The cells were lysed by sonication and then the supernatant (Sup.) was subjected to centrifugation. The insoluble cell debris (Pel.) was subjected to affinity chromatography. The first collected fraction was the void volume (Fth.), followed by the fraction after washing the resin by washing buffer 1 (W1) or washing buffer 2 (W2). The GR was collected after eluting by elution buffer 1 (E1) or elution buffer 2 (E2).

Table 4. The purification table of the glutathione reductase enzyme. The assay was carried out to determine the activity of the GR.

Stages	Volume (mL)	Protein (mg/mL)	Total protein (mg)	Conc. (U/mL)	Specific ctivity (U/mg)	Total activity (U)	Yield (%)	Fold
Crude	20	3.6	72	0.932	0.2588	18.64	100	1
Pure GR	4	1.1	4.4	0.337	0.3063	1.348	7.23	1.18

imperative to develop a procedure for high-level expression and effective purification of target proteins. The addition of a hexahistidine sequence at the C-terminal end of the recombinant protein does not influence the functional properties of the enzyme (33). The GR obtained in this study exhibited high purity and a subunit molecular weight of approximately 45 kDa; this result is consistent with those of previous studies, which reported wide variation in molecular weights among taxa. Mehul et al. (34) reported that GR from *Enterococcus faecalis* is 51.545 kDa. Bilge et al. (35) found that purified GR from rainbow trout is 50 kDa. Erat et al. (34) purified GR from chicken livers and observed a molecular weight of 43 kDa. William et al. (35) showed that GR isolated from the liver of the anoxia-tolerant turtle *Trachemys scripta elegans* is approximately 55 kDa. However, the molecular mass of GR in this study was not consistent with that of a previous study (29), which purified GR from camel erythrocytes and reported a subunit molecular weight of 60 kDa. This difference may due to differences in procedures. In this study the primers of recombinant GR did not have transit peptides in the N-terminal; therefore, the molecular weight was affected. On the other hand, the purified GR from camel erythrocytes in the previously mentioned study (29) was extracted as the entire enzyme, and that may reflect the difference in molecular weights.

There were also significant differences in the kinetic properties of GR derived from *C. dromedarius* and other sources. With respect to substrate affinity, the lower K_m value observed for GSSG than NADPH indicated that GR has a higher affinity to GSSG than NADPH. Similar results have been reported for GR isolated from other sources, such as rainbow trout livers, for which K_m values were 25 µM and 55 µM for GSSG and NADPH, respectively (35). Using GR from camel erythrocytes, the K_m values for GSSG and NADPH were 35.5 µM and 7.06 µM, respectively (29). Only GR derived from *Xanthomonas* species has the ability to use both NADPH and NADH as electron donors to reduce GSSG. The binding of human GR to NADH has lower affinity than binding to NADPH (9).

Purified GR exhibited maximum activity at a pH of 7, consistent with the results of other studies in which the optimal pH typically ranged from 6.5 to 8. However, GR exhibited maximum activity at 35 °C, which is different

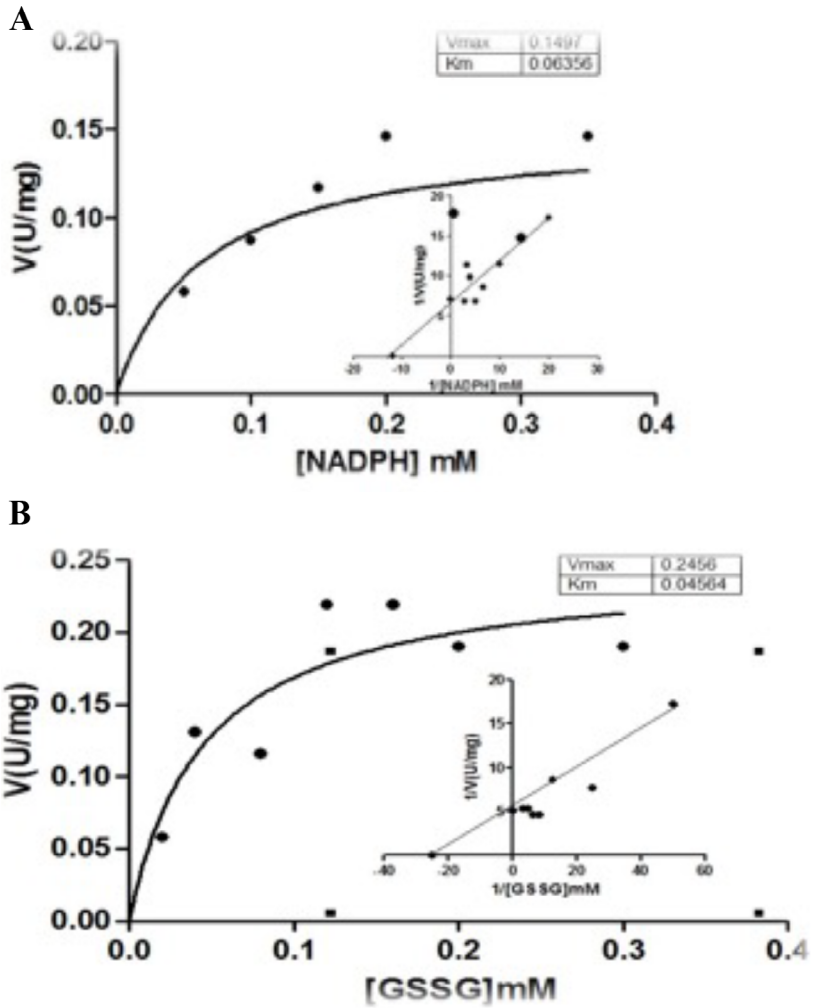

Figure 7. Michaelis–Menten curve and Lineweaver–Burk plot of GR activity in the presence of different concentrations of (A) NADPH and (B) GSSG as variable substrates.

from the optimum temperatures reported for GRs from different sources. For example, GR from *Phaeodactylum tricornutum* shows maximum activity at 32 °C (36). GR from rainbow trout liver shows maximum activity at 10 °C (35). Erat et al. (37) reported that chicken liver GR experienced maximum activity at 50 °C. These differences may reflect interspecific variation or a different adaptive mechanism for GR from the *C. dromedarius* liver.

GR is stable at temperatures of up to 70 °C. Many studies have shown that GR has mitochondrial antioxidant activity under heat exposure (38–42). However, in this study, the enzyme was stable at up to 50 °C, indicating that GR from the *C. dromedarius* liver is not stable at high temperatures, and this recombinant enzyme may have mediated stress responses differently among species. It would be useful to examine the thermostability of the enzyme over time in future studies. For example, a previous study (29) reported that GR purified from camel erythrocytes is stable at 70 °C for nearly 1 h, which was not consistent with the results of this study. In summary, the GR enzyme in camels has unique characteristics, e.g., its optimal temperature and pH, molecular weight, and substrate affinities. These partial characteristics are presumably related to the ability of camels to cope with harsh environmental conditions. Additional studies are required to determine precisely how the unique catalytic characteristics of GR are related to the acclimatization of *C. dromedarius* to harsh environmental conditions. The expression of GR from the camel liver in mammalian cells exposed to desert conditions may provide insight into the role of GR. We did not examine the inhibition of the purified enzyme, and such analyses may provide insight into the effects of extreme environmental conditions on enzyme activity.

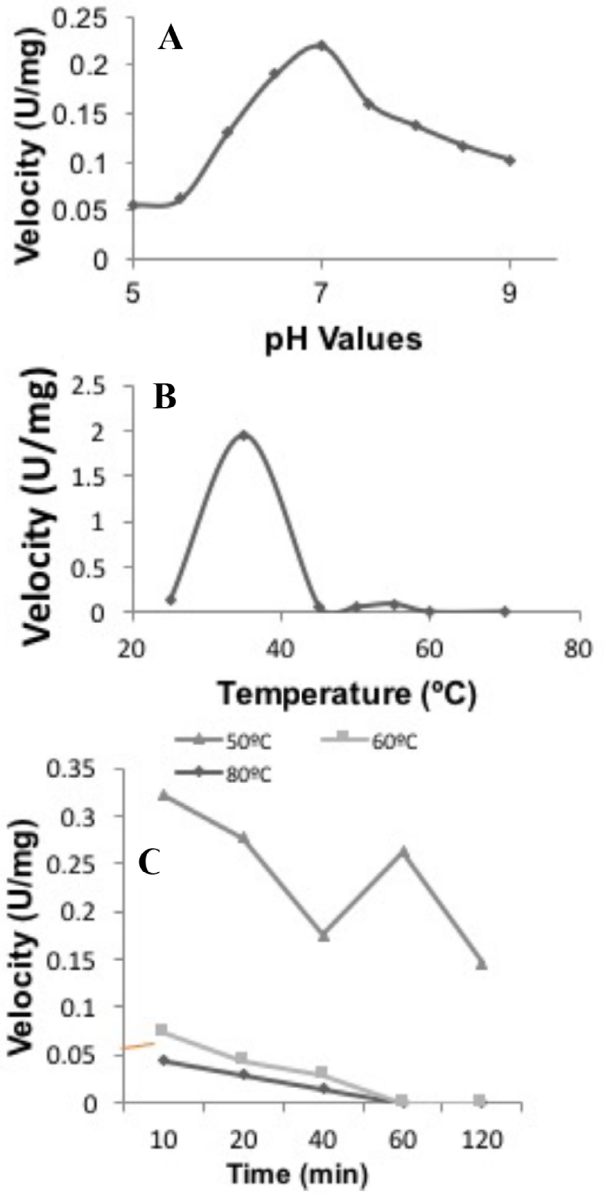

Figure 8. Effect of (A) pH, (B) temperature, and (C) different high temperatures on the relative activity of recombinant GR (U/mg).

Acknowledgments

We thank the Biochemistry Department at King Saud University, Riyadh, Saudi Arabia, for their support, especially the staff of the Protein Research Chair for the constant advice, technical assistance, critical comments, and valuable suggestions. We thank the Core Sequencing Facility at King Faisal Specialist Hospital and Research Center, Riyadh, Saudi Arabia, for *Gsr* sequencing. We thank Professor Arjumand S Warsy (Biochemistry Department, King Saud University) for his valuable contributions in the bioinformatics analysis. This work was funded by the Research Center of the Female Scientific and Medical Colleges, Deanship of Scientific Research, King Saud University, and the King Abdul-Aziz City for Science and Technology, Riyadh, Saudi Arabia.

References

1. Schirmer R, Krauth-Siegel RL. In: Dolphin D, Poulson R, Avramovic O, editors. Coenzymes and Cofactors: Glutathione. Hoboken, NJ, USA: John Wiley and Sons; 1989.
2. Kanzok SM, Fechner A, Bauer H, Ulschmid JK, Müller HM, Botella-Munoz J, Schneuwly S, Schirmer R, Becker K. Substitution of the thioredoxin system for glutathione reductase in *Drosophila melanogaster*. Science 2001; 291: 643-646.
3. Ridderstro M, Mannervik B. Optimized heterologous expression of the human zinc enzyme glyoxalase I. Biochem J 1996; 314: 463-467.
4. Szarka CE, Pfeiffer GR, Hum ST, Everley LC, Balshem AM, Moore DF, Litwin S, Goosenberg EB, Frucht H, Engstrom PF et al. Glutathione S-transferase activity and glutathione S-transferase expression in subject with risk for colorectal cancer. Cancer Res 1995; 55: 2789-2793.
5. Suvit L, Wirongrong W, Skorn M. The unique glutathione reductase from *Xanthomonase compestris*: gene expression and enzyme characterization. Biochem Biophys Res Commun 2005; 331: 1324-1330.
6. Chandra M. Metabolic function and molecular structure of glutathione reductase. Pharm Sci 2011; 9: 104-111.
7. Arscotte L, Veine D, Williams C. Disulfide with glutathione as an intermediate in the reaction catalyzed by glutathione reductase from yeast and as a major from of the enzyme in the cell. Biochemistry 2000; 39: 4711-4721.
8. Gul M, Kutay F, Temocin S, Hanninen O. Cellular and clinical implications of glutathione. Indian J Exp Biol 2000; 38: 625-634.
9. Ding Y, Miao J. Purification and characterization of a psychrophilic glutathione reductase from Antarctic ice microalgae *Chlamydomonas* sp. strain ICE-L. Polar Biol 2007; 31: 23-30.
10. Dhindsa R. Drought stress, enzyme of glutathione metabolism, oxidative injury and protein synthesis in *Tortula ruralis*. Plant Physiol 1991; 95: 648-651.
11. Tandoğan B, Ulusu NN. Kinetic mechanism and molecular properties of glutathione reductase. FABAD Journal of Pharmaceutical Sciences 2006; 31: 230-237.
12. Hargreaves P, Sheena Y, Land J, Heales S. Glutathione deficiency in patients with mitochondrial disease: implications for pathogenesis and treatment. J Inherit Metab Disord 2005; 28: 81-88.
13. Deponte M. Glutathione catalysis and the reaction mechanisms of glutathione-dependent enzymes. Biochim Biophys Acta 2013; 1830: 3217-3266.
14. Carlberg I, Mannervik B. Purification and characterization glutathione reductase from calf liver. An improved procedure for affinity chromatography on 2',5'-ADP Sepharose 4B. Anal Biochem 1981; 116: 531-536.
15. Le Trang N, Bhargava K, Cerami A. Purification of glutathione reductase from gerbil liver in two steps. Anal Biochem 1983; 133: 94-99.
16. Krohne G, Schirmer R, Untucht R. Glutathione reductase from human erythrocytes. Isolation of the enzyme and sequence analysis of the redox-active peptide. Eur J Biochem 1977; 80: 65-71.
17. Acan N, Tezcan E. Sheep brain glutathione reductase: purification and general properties. FEBS Lett 1989; 250: 72-74.
18. Ulusu G, Erat M, Çiftçi M, Şakiroğlu H, Bakan E. Purification and characterization of glutathione reductase from sheep liver. Turk J Vet Anim Sci 2005; 29: 1109-1117.
19. Taşer P, Çiftçi M. Purification and characterization of glutathione reductase from turkey liver. Turk J Vet Anim Sci 2012; 36: 546-553.
20. Takeda T, Ishikawa T, Shigeoka S, Hirayama O, Mitsunaga T. Purification and characterization of glutathione reductase from *Chlamydomonas reinhardtii*. Microbiology 1993; 139: 2233-2238.
21. Cleere W, Coughlan M. Avian xanthine dehydrogenases-I. Isolation and characterization of the turkey liver enzyme. Comp Biochem Physiol 1975; 15: 311-322.
22. Toribio F, Martinez E, Pascual P, Lopez J. Methods for purification of glutathione peroxidase and related enzymes. J Chromatogr B 1996; 684: 77-97.
23. Brodelius P, Larsson P, Mosbach K. The synthesis of three AMP-analogues: N6-(6-aminohexyl)-adenosine 5'-monophosphate, N6-(6-aminohexyl)-adenosine 2',5'-bisphosphate, and N6-(6-aminohexyl)-adenosine 3',5'-bisphosphate and their application as general ligands in biospecific affinity chromatography. Eur J Biochem 1974; 47: 81-89.
24. Mannervik B, Jacobsson K, Boggaram V. Purification of glutathione reductase from erythrocytes by the use of affinity chromatography on 2',5'-ADP-Sepharose 4-B. FEBS Lett 1976; 66: 221-224.
25. Sambrook J, Fritschi EF, Maniatis T. Molecular Cloning: A Laboratory Manual. 2nd ed. Cold Spring Harbor, NY, USA: Cold Spring Harbor Laboratory Press; 1989.
26. Larkin MA, Blackshields G, Brown NP, Chenna R, McGettigan PA, McWilliam H, Valentin F, Wallace IM, Wilm A, Lopez R et al. ClustalW and ClustalX version 2. Bioinformatics 2007; 23: 2947-2948.
27. Laemmli U. Cleavage of structural proteins during the assembly of the head of bacteriophage T4. Nature 1970; 227: 680-685.
28. Caarlberg I, Mannervik B. Purification and characterization of the flavoenzyme glutathione reductase from rat liver. J Biol Chem 1975; 250: 5475-5480.
29. Alsenaidy A. Purification and characterization of glutathione reductase from camel (*Camelus dromedaries*) erythrocytes. Eur J Sci Res 2010; 48: 142-154.

30. Bradford M. A rapid and sensitive method for the quantitation of microgram quantities of protein utilizing the principle of protein-dye binding. Anal Biochem 1976; 72: 248-254.

31. Wu G, Fang Y, Yang S, Lupton J, Turner N. Glutathione metabolism and its implications for health. J Nutr 2004; 134: 489-492.

32. Ridderström M, Mannervik B. Optimized heterologous expression of the human zinc enzyme glyoxalase I. Biochem J 1976; 314: 463-467.

33. Serrano A, Rivas J, Losada M. Purification and properties of glutathione reductase from the cyanobacterium *Anabaena* sp. strain 7119. Bacteriology 1984; 158: 317-324.

34. Patel MP, Marcinkeviciene J, Blanchard JS. *Enterococcus faecalis* glutathione reductase: purification, characterization and expression under normal and hyperbaric O_2 conditions. FEMS Microbiol Lett 1998; 166: 155-163.

35. Tekman B, Ozdemir H, Senturk M, Ciftci M. Purification and characterization of glutathione reductase from rainbow trout (*Oncorhynchus mykiss*) liver and inhibition effect of metal ion on enzyme activity. Comp Biochem Physiol 2008; 148: 117-121.

36. Arias DG, Marquez VE, Beccaria AJ, Guerrero SA, Iglesias AA. Purification and characterization of glutathione reductase from *Phaeodactylum tricornutum*. Protist 2010; 161: 19-101.

37. Erat M, Demir H, Şakiroğlu H. Purification of glutathione reductase from chicken liver and investigation of kinetics properties. Appl Biochem Biotech 2005; 125: 127-138.

38. Willmore W, Storey K. Purification and properties of glutathione reductase from liver of the anoxia-tolerant turtle, *Trachemys scripta elegans*. Mol Cell Biochem 2006; 297: 139-149.

39. Stojkovski V, Hadzi-Petrushev N, Ilieski V, Sopi R, Gjorgoski I, Mitrov D, Jankulovski N, Mladenov M. Age and heat exposure-dependent changes in antioxidant enzymes activities in rat's liver and brain mitochondria: role of alpha-tocopherol. Physiol Res 2013; 62: 503-510.

40. Dorts J, Bauwin A, Kestemont P, Jolly S, Sanchez W, Silvestre F. Proteasome and antioxidant responses in *Cottus gobio* during a combined exposure to heat stress and cadmium. Comp Biochem Phys B 2012; 155: 318-324.

41. Kaur M, Atif F, Ansari RA, Ahmad F, Raisuddin S. The interactive effect of elevated temperature on deltamethrin-induced biochemical stress responses in *Channa punctata* Bloch. Chem Biol Interact 2011; 193: 216-224.

42. Malik AI, Storey KB. Activation of antioxidant defense during dehydration stress in the African clawed frog). Gene 2009; 442: 99-107.